

ical review of the literature; approval of the final version of the manuscript.

Milene Cripa Pizzato de Araújo: Data collection, or analysis and interpretation of data; drafting and editing of the manuscript or critical review of important intellectual content; collection, analysis and interpretation of data; critical review of the literature; approval of the final version of the manuscript.

Victória Prudêncio Ferreira: Data collection, or analysis and interpretation of data; drafting and editing of the manuscript or critical review of important intellectual content; collection, analysis and interpretation of data; critical review of the literature; approval of the final version of the manuscript.

Jessica Almeida Marani: Data collection, or analysis and interpretation of data; drafting and editing of the manuscript or critical review of important intellectual content; collection, analysis and interpretation of data; critical review of the literature; approval of the final version of the manuscript.

Airton dos Santos Gon: Design and planning of the study; statistical analysis; drafting and editing of the manuscript or critical review of important intellectual content; collection, analysis and interpretation of data; intellectual participation in the propaedeutic and/or therapeutic conduct of the studied cases; critical review of the literature; approval of the final version of the manuscript.

## Conflicts of interest

None declared.

## References

1. Tso S, Satchwell F, Moiz H, Hari T, Dhariwal S, Barlow R, et al. Erythroderma (exfoliative dermatitis). Part 1: underlying causes, clinical presentation and pathogenesis. *Clin Exp Dermatol.* 2021;46:1001–10.
2. Akhyani M, Ghodsi ZS, Toosi S, Dabbaghian H. Erythroderma: a clinical study of 97 cases. *BMC Dermatol.* 2005;5:5.

3. Fernandes NC, Pereira FSM, Maceira JP, Cuzzi T, Dresch TFLR, Araújo PP. Eritrodermia: estudo clínico-laboratorial e histopatológico de 170 casos. *An Bras Dermatol.* 2008;83:526–32.
4. Tan GF, Kong YL, Tan AS, Tey HL. Causes and features of erythroderma. *Ann Acad Med Singap.* 2014;43:391–4.
5. Cesar A, Cruz M, Mota A, Azevedo F. Erythroderma. A clinical and etiological study of 103 patients. *J Dermatol Case Rep.* 2016;10:1–9.
6. Miyashiro D, Sanches JA. Erythroderma: a prospective study of 309 patients followed for 12 years in a tertiary center. *Sci Rep.* 2020;10:9774.
7. Carrasquillo OY, Pabón-Cartagena G, Falto-Aizpurua LA, Santiago-Vázquez M, Cancel-Artau KJ, Arias-Berrios G, et al. Treatment of erythrodermic psoriasis with biologics: a systematic review. *J Am Acad Dermatol.* 2020;83:151–8.
8. Pereyra-Rodriguez JJ, Dominguez-Cruz J, Armario-Hita JC, Villaverde RR. 104-week safety and effectiveness of dupilumab in the treatment of severe atopic dermatitis. The experience of 5 reference dermatology units in Spain. *An Bras Dermatol.* 2021;96:787–90.
9. Hama N, Abe R, Gibson A, Phillips EJ. Drug-induced hypersensitivity syndrome (DIHS)/drug reaction with eosinophilia and systemic symptoms (DRESS): clinical features and pathogenesis. *J Allergy Clin Immunol Pract.* 2022;10:1155–67.
10. Zazzara MB, Palmer K, Vetrano DL, Carfi A, Onder G. Adverse drug reactions in older adults: a narrative review of the literature. *Eur Geriatr Med.* 2021;12:463–73.

Rogério Nabor Kondo , Betina Samesima e Singh , Milene Cripa Pizzato de Araújo , Victória Prudêncio Ferreira , Jessica Almeida Marani , Airton dos Santos Gon 

Department of Internal Medicine, Universidade Estadual de Londrina, Londrina, PR, Brazil

\* Corresponding author.

E-mail: [kondo.dermato@gmail.com](mailto:kondo.dermato@gmail.com) (R.N. Kondo).

Received 3 May 2023; accepted 10 July 2023

<https://doi.org/10.1016/j.abd.2023.07.014>

0365-0596/ © 2024 Sociedade Brasileira de Dermatologia.

Published by Elsevier España, S.L.U. This is an open access article under the CC BY license (<http://creativecommons.org/licenses/by/4.0/>).

## Insulin inhibits melanoma tumor growth through the expression of activating transcription factor 4, without detectable expression of transcription factor CHOP: an *in vivo* model\*



Dear Editor,

In the first half of the 20<sup>th</sup> century, there were reports<sup>1</sup> of size reduction in different types of tumors treated with high

doses of insulin, including a case of metastatic melanoma.<sup>2</sup> As these treatments induced hypoglycemic states<sup>2</sup> and due to the close relationship between neoplasms and glycemia,<sup>3</sup> it was concluded that this response occurred due to patients low blood glucose levels. However, the mechanism of this interaction seems to be the expression of activating transcription factor 4 (ATF4) and other associated proteins, such as transcription factor CHOP (TFCHOP).

Therefore, the present study aims to demonstrate the effects of insulin administered to mice with melanoma, the relationship between the tumor response and blood glycemia and the protein expression possibly involved in this mechanism.

All procedures were approved by the Animal Use Ethics Committee (number 23075.067738/2019-05). Murine melanoma cell lines (B16-F10) were obtained from ATCC (American Type Culture Collection, Manassas, VA, USA),

\* Study conducted at the Extracellular Matrix and Poison Biotechnology Laboratory, Department of Cell Biology, Universidade Federal do Paraná, Curitiba, PR, Brazil.

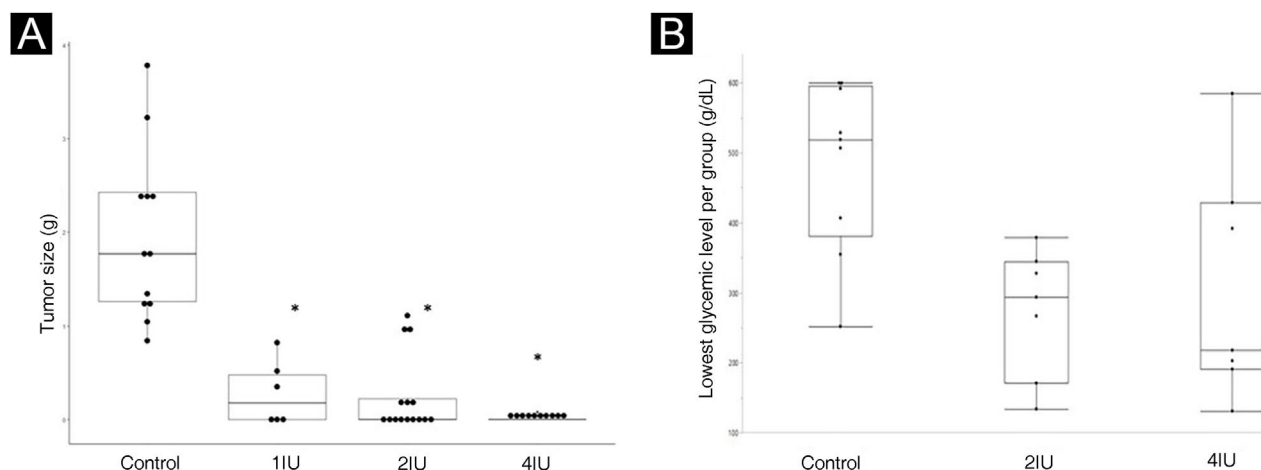


**Figure 1** Insulin inhibits tumor growth in a murine model of melanoma (C57BL6/B16F10), without causing hypoglycemia. (A) Boxplot representing the average size of tumors excised in each experimental group. Statistical evaluation was performed using the Kruskal-Wallis test, followed by Dunn's test. (B) Boxplot representation of glycemic levels measured in mice. The 1IU group did not have blood glucose levels assessed due to the fact that it was a standard dose used in medical practice. The lowest blood glucose levels, in any of the groups, were not below 136 mg/dL, showing the absence of hypoglycemia in the mice. \* p value < 0.05 in relation to the control group.

cultured in DMEM medium, and injected subcutaneously ( $6 \times 10^6$  cells per animal) into male C57BL/6 mice, aged eight to 12 weeks (obtained from Instituto Carlos Chagas, Fiocruz – Paraná), totaling 50 animals. The mice were fed a standard diet (Purina) during the experiments. After five days, the development of a solid tumor of variable size was observed at the site of application. Regular human insulin 100 IU/mL (Novolin R<sup>®</sup>) was used to treat the animals, diluted in 50% glucose solution. The mice were divided into four groups according to the treatment scheme: 15 mice in the control group (0.1 mL of 50% glucose solution); ten mice in the 1IU/kg group (0.1 mL of solution at 0.1 IU/mL); ten mice in the 2IU/kg group (0.1 mL of solution at 0.2 IU/kg); and 15 mice in the 4IU/kg group (0.1 solution at 0.4 IU/mL). Insulin was administered intraperitoneally for a total of 15 days, divided into three cycles of five days, with two-day intervals without hormone administration (Supplementary Material 1). Glycemic levels were measured using a glucose meter (Accu Check Active, Roche Diagnostic, Germany), using a blood sample obtained through a small cut in the tail. The collection occurred only in the control, 2IU, and 4IU groups, three times a week. After the end of treatment, the animals were euthanized using a combination of xylazine hydrochloride and ketamine hydrochloride (10%) in 50 mL (1:1).

Tumor tissue was extracted and the immunohistochemical analysis was performed using slides of tumor sections from B16-F10 tumors obtained from *in vivo* experiments. Immunohistochemistry slides were prepared according to the indexed protocol (Supplementary Material 2) using the primary antibodies: anti-TFCHOP for rats (Santa Cruz Biotechnology, cat.sc 7351) and anti-ATF4 for rats, (Santa Cruz Biotechnology, cat. sc 390063). Immunohistochemical quantification was performed using the "ImageJ Analysis Software" program, according to the Crowe and Yue protocol.<sup>4</sup> Control slides were used to determine basic parameters and as a reference for relative expression. The

immunohistochemistry positivity area and the number of nuclei per evaluated slide field were also assessed. Three  $\times 20$  magnification fields per slide were used for the analysis.

The statistical analysis and graphs were carried out using the R program (R Development Core Team). A comparison was performed using the Kruskal-Wallis test and revised using Dunn's test for tumor sizes and protein expression, nuclei count and stained area on the slides. Glycemic levels were not included in the statistical analysis, since the aim of the study was not to demonstrate differences between the groups regarding this variable, but rather the absence of severe hypoglycemia.

The effects of insulin *in vivo* were analyzed using the animal model, measuring the size of the tumors at the end of the treatment. The box-plot graph of the size of the tumors is shown in Fig. 1A, while the glycemic levels obtained in the animals are shown in Fig. 1B, considering the reference value for mice (150 mg/dL).

The number of animals that died during the experiments comprised two in the control group and four in the 1IU/kg group. Deaths were due to tumor progression in the animals. These deaths were observed throughout the second week of the experiments and the tumors of these animals were not analyzed.

The expression of ATF4 (Fig. 2A and B) was increased in the 2IU/kg and 4IU/kg groups when compared to the control group, with statistical significance. The images obtained to evaluate TFCHOP (Fig. 2C and D) showed a statistical difference in the 4IU group when compared to the control group (Fig. 3). In the qualitative analysis of the slides, a lower count of nuclei was observed in the treated groups and a larger stained area in the 4IU (ATF4) and 1IU (TFCHOP) groups (Table 1).

Although modern literature establishes a neoplastic role for insulin, so that the hormone use is related to tumor emergence/growth,<sup>5,6</sup> the present study is supported by data from the beginning of the 20<sup>th</sup> century,<sup>1</sup> in which

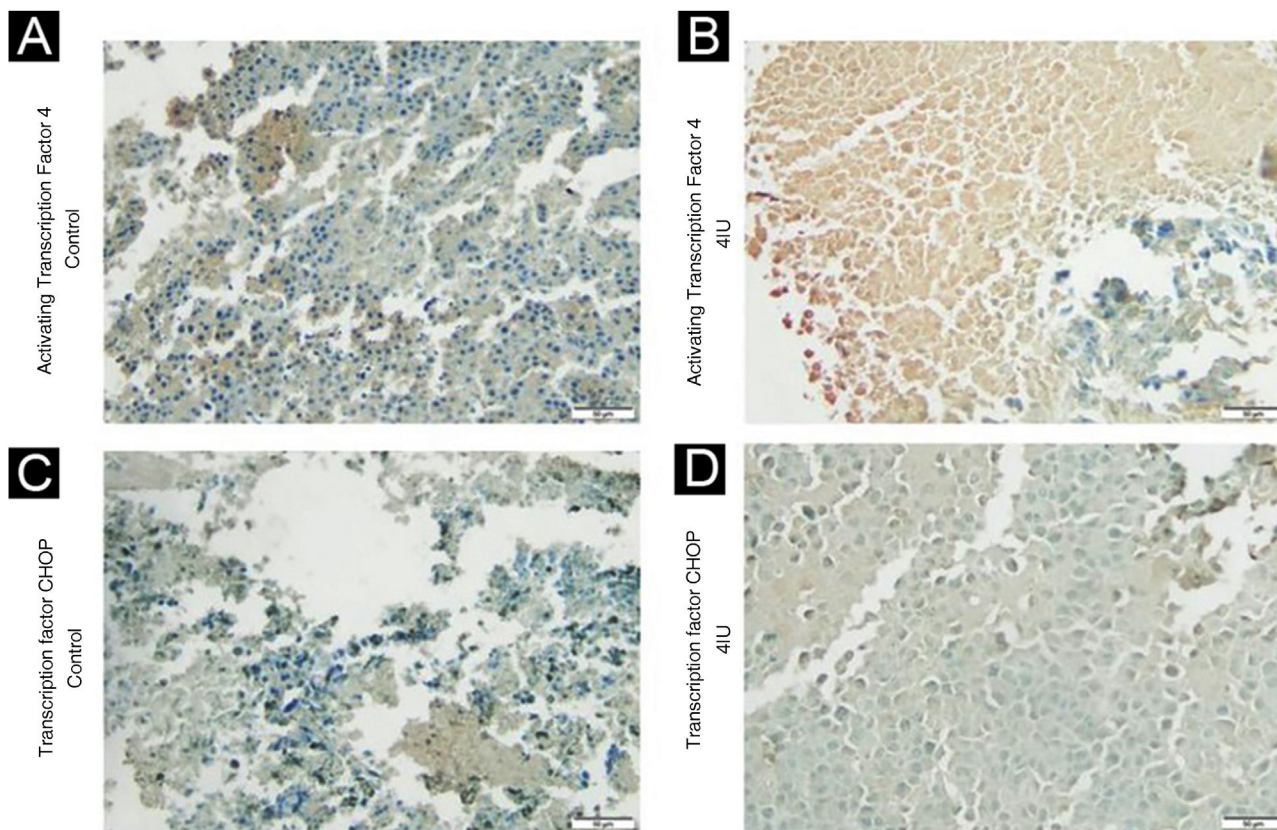


**Figure 2** Immunohistochemical analysis of ATF4 and TFCHOP expression. Tissues obtained from tumor material from the control (A and C) and 4 IU/kg (B and D) groups were evaluated based on the immunohistochemical expression of these proteins. The photographs were obtained using an Axiolab 5 microscope (Zeiss) and analyzed using the ImageJ FIJI software program. The control and 4 IU/kg groups were chosen to represent dose extremes.

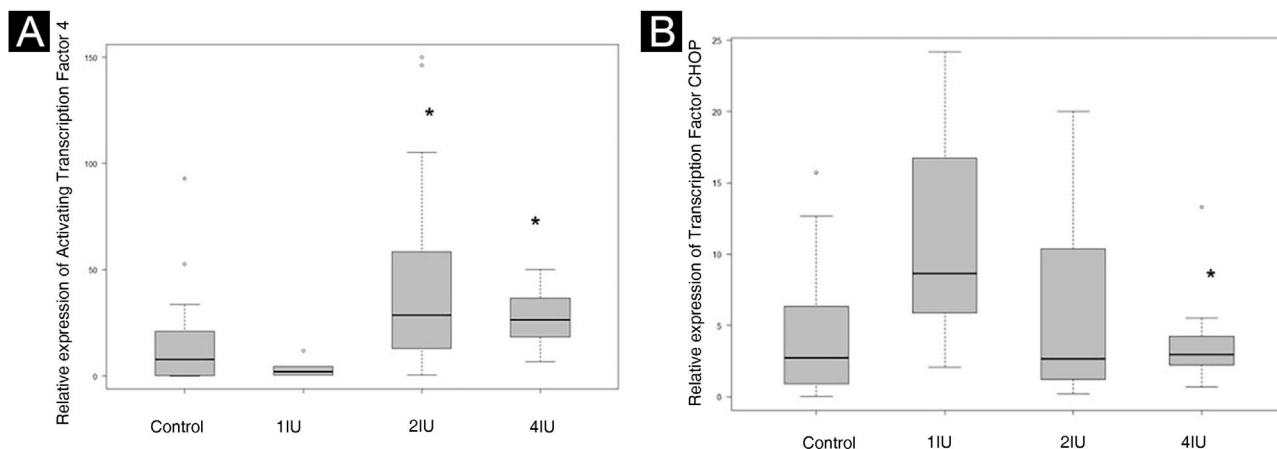


**Figure 3** Relative expression of ATF4 and TFCHOP. Control slides were used to define the comparison parameters. (A) Quantification of the signal expressed by ATF4 in slides from different groups. (B) Quantification of the signal expressed by TFCHOP in slides from different groups. The dispersion of relative values was represented on the graph. Statistical evaluation was performed using the Kruskal-Wallis test, followed by Dunn's test. \* p value < 0.05 in relation to the control group.

it was demonstrated that insulin showed antineoplastic activity.

The insulin-mediated protein expression of ATF4, rather than hypoglycemia, seems to be related to antineoplastic action. ATF4 plays a dual role within the cell in situations of endoplasmic reticulum stress (ERS),<sup>7</sup> promoting

cell survival or initiating apoptosis, mainly through the PERK/eIF2a/ATF4/TFCHOP pathway. The literature stipulates that insulin is linked to ATF4 expression in healthy<sup>8</sup> and tumor cells<sup>9</sup> and these data are corroborated by the findings of the present article. The expression of TFCHOP only in the 4IU group may be related to the amount of tumor material

**Table 1** Immunohistochemical analysis of the expression of transcription factor CHOP and activating transcription factor 4 in tissues obtained from 1 IU/kg, 2 IU/kg and 4 IU/kg groups tumors. The data showed a lower number of nuclei in the groups treated with insulin, while a larger stained area was only observed in the evaluation of ATF4 and the 1IU group of TFCHOP. The p-value obtained by the Kruskal-Wallis test is represented in the last column, and values with a significant difference from the control group ( $p < 0.05$ ) are marked with an asterisk.

	Control	1IU	2IU	4IU	p-value
<b>IHC Positive Area Average</b>					
ATF4	7.6%	2.0%	20.0%*	14.17%*	>0.05
<b>Number of nuclei per slide (average)</b>					
ATF4	1614	1345.7	721.0*	114.5*	>0.05
<b>IHC Positive Area Average</b>					
TFCHOP	1.7%	4.4%*	2.4%	1.5%	>0.05
<b>Number of nuclei per slide (average)</b>					
TFCHOP	2391	661.7*	785.9*	127.20*	>0.05

in the slides of the 2IU group, observed by the stained percentage, as well as by other pathways for inducing apoptosis in cells, such as the TRAIL protein.<sup>10</sup>

The limitations of the present study include the fact that it did not assess whether the tumors would become refractory to insulin use or whether there would be recurrences. Animal weight, the possible increase in body mass in the groups treated with insulin, animals survival time after treatment, or the presence of other cell markers that could be involved in the processes, such as the TRAIL protein, were not evaluated. Another limitation is the evaluation of protein expression using immunohistochemical slides.

### Financial support

None declared.

### Authors' contributions

Daniel do Prado: Design of the study; developed the theory behind the experiments; planned the study; drafting and editing of the manuscript; performed the statistical analysis and analyzed the data.

Marianna Boia: Performed the experiments; contributed to sample preparation and data interpretation.

Hanna Camara da Justa: Participated in the experiments.

Andrea Senff Ribeiro: Contributed to the interpretation of the results and supervised the project.

Sergio Lunardon Padilha: Contributed to the interpretation of the results and supervised the project.

### Conflicts of interest






None declared.

### Appendix A. Supplementary material

Supplementary material related to this article can be found, in the online version, at doi:<https://doi.org/10.1016/j.abd.2023.07.012>.

### References

- Klement RJ. Wilhelm Brünings' forgotten contribution to the metabolic treatment of cancer utilizing hypoglycemia and a very low carbohydrate (ketogenic) diet. *J Tradit Complement Med.* 2018;9:192–200, <http://dx.doi.org/10.1016/j.jtcme.2018.06.002>.
- Koroljow S. Two cases of malignant tumors with metastases apparently treated successfully with hypoglycemic coma. *Psychiatr Q.* 1962;36:261–70, <http://dx.doi.org/10.1007/BF01586115>.
- Bose S, Zhang C, Le A. Glucose metabolism in cancer: the Warburg effect and beyond. *Adv Exp Med Biol.* 2021;1311:3–15, [http://dx.doi.org/10.1007/978-3-030-65768-0\\_1](http://dx.doi.org/10.1007/978-3-030-65768-0_1).
- Crowe AR, Yue W. Semi-quantitative determination of protein expression using immunohistochemistry staining and analysis: an integrated protocol. *Bio Protoc.* 2019;9:e3465, <http://dx.doi.org/10.21769/BioProtoc.3465>.
- Leitner BP, Siebel S, Akingbesote ND, Zhang X, Perry RJ. Insulin and cancer: a tangled web. *Biochem J.* 2022;479:583–607, <http://dx.doi.org/10.1042/BCJ20210134>.
- Chieffari E, Mirabelli M, La Vignera S, Tanyolac S, Foti DP, Aversa A, et al. Insulin resistance and cancer: in search for a causal link. *Intl J Mol Sci.* 2021;22:11137, <http://dx.doi.org/10.3390/ijms22011137>.
- Rozpedek W, Pytel D, Mucha B, Leszczynska H, Diehl JA, Majsterek I. The role of the PERK/eIF2 $\alpha$ /ATF4/CHOP signaling pathway in tumor progression during endoplasmic reticulum stress. *Curr Mol Med.* 2016;16:533–44, <http://dx.doi.org/10.2174/1566524016666160523143937>.
- Adams CM. Role of the transcription factor ATF4 in the anabolic actions of insulin and the antianabolic actions of glucocorticoids. *J Biol Chem.* 2007;282:16744–53, <http://dx.doi.org/10.1074/jbc.M610510200>.
- Inageda K. Insulin modulates induction of glucose-regulated protein 78 during endoplasmic reticulum stress via augmentation of ATF4 expression in human neuroblastoma cells. *FEBS Lett.* 2010;584:3649–54, <http://dx.doi.org/10.1016/j.febslet.2010.07.040>.
- Iurlaro R, Püschel F, León-Annichiarico CL, O'Connor H, Martin SJ, Palou-Gramón D, et al. Glucose deprivation induces ATF4-mediated apoptosis through TRAIL death receptors. *Mol Cell Biol.* 2017;37:e00479–16, <http://dx.doi.org/10.1128/MCB.00479-16>.

Daniel do Prado <sup>a,\*</sup>, Marianna Boia-Ferreira <sup>b</sup>,  
Hanna Camara da Justa <sup>b</sup>, Andrea Senff-Ribeiro <sup>b</sup>,  
Sérgio Lunardon Padilha <sup>a</sup>

<sup>a</sup> Department of Internal Medicine, Universidade Federal do Paraná, Curitiba, PR, Brazil

<sup>b</sup> Department of Cell Biology, Universidade Federal do Paraná, Curitiba, PR, Brazil

\* Corresponding author.

E-mail: [danieldoprado1@gmail.com](mailto:danieldoprado1@gmail.com) (D. do Prado).

Received 21 February 2023; accepted 3 July 2023

<https://doi.org/10.1016/j.abd.2023.07.012>

0365-0596/ © 2024 Published by Elsevier España, S.L.U. on behalf of Sociedade Brasileira de Dermatologia. This is an open access article under the CC BY license (<http://creativecommons.org/licenses/by/4.0/>).

## Predicting skin graft failure on the scalp by intraoperative laser speckle analysis<sup>☆</sup>



Dear Editor,

Reconstruction with skin grafts after cutaneous malignancy excision might carry some graft failure despite the best surgical practice.<sup>1,2</sup> It is well-established that a poorly perfused recipient bed has a higher risk of skin graft failure.<sup>3</sup>

The vascular supply for skin grafts on the scalp derives mainly from aponeurotic galea, but in a dermatologic setting, its integrity is often compromised.<sup>4</sup> By week four, the failure rate of full-thickness skin grafts (FTSG) on the scalp can reach 22%.<sup>1</sup>

The impact of the perfusion status of the recipient bed on graft viability at week four still needed to be quantified in humans *in vivo*.<sup>3</sup>

Laser speckle contrast imaging (LSCI) is a non-invasive, real-time, contactless technique that allows the study of microcirculation on large surface areas intra- and perioperatively.<sup>5</sup> In previous research, we validated the study of microcirculation of distinct types of skin grafts by LSCI analysis.<sup>6</sup> Its role in identifying high-risk patients for graft necrosis still needs to be explored.

In this pilot study, we aim to compare the outcomes of FTSG on the scalp with the baseline graft bed perfusion assessed by LSCI. We will also describe the changes in FTSG perfusion over four weeks.

After local ethics committee approval and informed consent, four consecutive patients with non-melanoma skin cancer of the scalp were enrolled: all male gender with 71y/o (patient 1), 90y/o (patient 2), 81y/o (patient 3) and 78y/o (patient 4). The main characteristics and comorbidities of the patients are presented in Table 1. The tumors were excised after lidocaine with epinephrine infiltration, and FTSG were harvested from the infraclavicular area. Twenty minutes after lesion removal and before skin graft suture, baseline wound bed perfusion (in arbitrary perfusion units, APU) was measured with LSCI for 1 minute, and mean arterial pressure (MAP, in mmHg) was registered. The ratio APU/MAP yielded cutaneous vascular conductance (CVC, in APU/mmHg), allowing the comparison of patients' perfusion

values. FTSG was ultimately sutured, and tie-over-dressing was applied for one week.

By day (D) 7, D14, D21, and D28, graft perfusion was assessed and compared with baseline perfusion of graft bed on D0. Clinical pictures were also registered. Necrosis areas were calculated with SketchAndCalc Area Calculator™ (version 6.2.5, 2018).

In all patients, skin cancer removal allowed the preservation of some underlying aponeurotic galea for skin graft vascular supply. No patient developed a postoperative infection, hematoma, or hemorrhage.

The primary defect areas were 8.4 cm<sup>2</sup> (patient 1), 12.3 cm<sup>2</sup> (patient 2), 5.8 cm<sup>2</sup> (patient 3), and 8.7 cm<sup>2</sup> (patient 4). The evolution of CVC values over the four weeks is represented in Fig. 1. The sequential clinical and LSCI images registered during the same period are presented in Fig. 2.

Baseline CVC values of the recipient bed were 0.22 APU/mmHg, 0.43 APU/mmHg, 0.51 APU/mmHg, and 0.70 APU/mmHg, respectively, on patients 1, 2, 3, and 4. The graft necrosis extension on day 28 decreased with increased recipient bed perfusion (CVC) on day 0. It was 82% on patient 1, 48% on patient 2, 16% on patient 3, and 9% on patient 4.

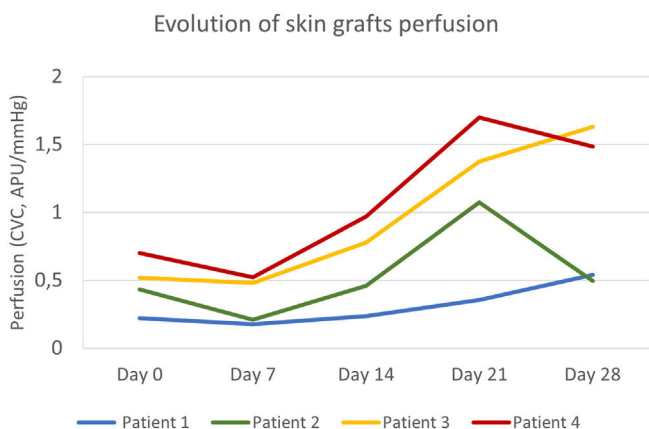


**Figure 1** Evolution of full-thickness skin grafts perfusion on the scalp. Skin graft perfusion on day 7 was lower than baseline graft bed perfusion in all patients. Patients 3 and 4 had higher baseline perfusion and reached peak values on day 21 and day 28, respectively. Patient 1, with the worst clinical outcome, had an ascending curve until day 28 but with persistently lower perfusion values.

<sup>☆</sup> Study conducted at the Dermatology Department of Hospital and University Centre of Coimbra, Coimbra, Portugal.